

Membranes with rotating motors: Microvortex assemblies

P. Lenz^{1,2,a}, J.-F. Joanny¹, F. Jülicher^{1,3}, and J. Prost^{1,4}

¹ Institut Curie, UMR 168, 26 rue d'Ulm, F-75248 Paris Cédex 05, France

² Fachbereich Physik, Philipps-Universität Marburg, D-35032 Marburg, Germany

³ Max-Planck-Institut für Physik komplexer Systeme, Nöthnitzer Straße 38, D-01187 Dresden, Germany

⁴ Ecole supérieure de physique et chimie industrielles, 10 rue Vauquelin, F-75231 Paris Cédex 05, France

Received 9 October 2003 /

Published online: 11 May 2004 – © EDP Sciences / Società Italiana di Fisica / Springer-Verlag 2004

Abstract. We study collections of rotatory motors confined to 2-dimensional manifolds. The rotational motion induces a repulsive hydrodynamic interaction between motors leading to a non-trivial collective behavior. For high rotation speed, motors should arrange on a triangular lattice exhibiting crystalline order. At low speed, they form a disordered phase where diffusion is enhanced by velocity fluctuations. In confining geometries and under suitable boundary conditions, motor-generated flow might enhance left-right symmetry-breaking transport. All these effects should be experimentally observable for motors driven by external fields and for dipolar biological motors embedded into lipid membranes in a viscoelastic solvent.

PACS. 87.16.-b Subcellular structure and processes – 05.40.-a Fluctuation phenomena, random processes, noise, and Brownian motion – 87.15.Kg Molecular interactions; membrane-protein interactions

1 Introduction

Motor proteins play an essential role in many cellular processes such as, *e.g.*, muscle contraction, chemotaxis, vesicular trafficking, chromosome segregation during cell division, etc. [1]. There is a variety of different motor proteins that can have either a translational or a rotational motion. The most important linear motors include kinesins or myosins and dyneins which move in a deterministic way along filaments (actin and microtubules, respectively) and transcription enzymes such as RNAPolymerases which follow nucleotide strands.

A prominent example of a rotating motor is adenosine triphosphate synthase (ATPsynthase). ATPsynthase is a large multisubunit protein, consisting of a large enzymatic protruding portion F_1 attached to a membrane-embedded, proton-conducting portion F_0 [2]. When protons flow through F_0 , ATP is synthesized in F_1 . It is thought [3–5] that the protons passing through the transmembrane carrier cause the stalk to spin rapidly within the head, inducing the head to make ATP. The motor is reversible and an excess of ATP provokes a rotation in the opposite direction and a reverse flux of protons.

Another system which can effectively behave as a rotating motor are cilia. Cilia are hair-like structures that extend from the surface of many kinds of eucaryotic cells. They are formed from specialized groupings of microtubules called “basal bodies”. Cells are able to generate

flow by utilizing cilia: their primary function is to move fluid over the surface of a cell or to propel single cells through a fluid. The beat cycles of cilia can be quite complicated [6], but they also can exhibit rotational motion [7]. In multiciliar arrays hydrodynamic interactions between neighboring cilia lead to cooperative beating patterns [8].

There are strong experimental indications that defect cilia might cause certain pathologies, the most prominent example being the disease called “*situs inversus*”. It has been shown [7] that the absence of functional cilia leads to randomization of the left-right placement of organs. However, by subjecting the surface of the embryos to an artificial flow, left-right patterning could be re-established in mice with only non-motile cilia [9]. Currently, several models are being discussed to explain the experimentally observed behavior [10–12]. In all these approaches the cilia-generated flow plays an essential role which triggers the symmetry-breaking event.

The situation is somewhat different for ATPsynthase. Its function is to synthesize ATP (or to build up gradients in proton concentration). Up to now, it is not known whether the hydrodynamic flow field caused by the rotational motion has a biological function. However, the hydrodynamic flow generated by these motors can change the properties of the membranes in which they are embedded and can, *e.g.*, enhance the diffusion of membrane proteins. Furthermore, these rotating motors are fascinating objects with a potential for technological applications.

^a e-mail: peter.lenz@physik.uni-marburg.de

The integration of arrays of biomolecular motors into nano-engineered structures could be used, *e.g.*, for the creation of a novel class of mobile nanodevices, sorting machines or force transducers [13].

The first realization of a motor-powered nanodevice was given by the group of Kinosita [5]. They attached actin filaments to the rotating stalk, observed its rotation and measured the torque exerted by the surrounding fluid on the motor. Subsequently, artificial systems were engineered consisting of a substrate-supported array to which F_1 -ATPase molecules were linked. Nanopropellers (150 nm in diameter and 750 to 1400 nm long) were attached to the rotating portion of F_1 [14]. It is envisioned that in such setups F_1 -ATPase motors can be used to create in a controlled fashion a hydrodynamic flow field which will provide mechanical drives for a new class of nanomechanical devices.

Both cilia and ATPsynthase are embedded into membranes. Thus, from a theoretical point of view, these systems are special realizations of active membranes, *i.e.* membranes containing active components. Recently, theoretical models have been introduced to describe the properties of these systems in situations where active processes driven by ATP hydrolysis, chemical gradients or light exert forces on the membrane [15]. Whereas the shapes and fluctuations of model fluid membranes at thermal equilibrium are by now well understood [16], the experimental and theoretical investigation of active membranes has just started. Up to now, studies have concentrated on membranes containing active pumps and channels [17,18]. It has been shown that non-equilibrium noise enhances the shape fluctuations of the membranes. Triggered by these investigations, a series of experiments has been carried out which has confirmed the theoretical predictions [19,20]. There are also indications that these theoretical ideas apply directly to simple biological systems such as red blood cells where non-equilibrium processes seem to influence the flickering [21–23].

The study of rotatory motors is not restricted to membrane-embedded molecules. As has been demonstrated by the group of Whitesides, magnetic disks can be confined to a liquid surface and then brought to rotation by an external magnetic field [24,25]. The observed pattern formation should also occur for rotors stirred by Laser tweezers [26]. It should be emphasized that these artificial motors are rotational monopoles driven by an external field while the biological macromolecules are driven by internally generated forces and correspond to rotational dipoles.

In a recent paper [27], we have studied rotational monopoles confined to a 2-dimensional manifold and dipolar motors embedded into membranes. We have shown that these systems exhibit, in contrast to membranes containing pumps and channels, a non-trivial collective behavior since the rotational motion may induce repulsive hydrodynamic interactions between motors. Consequently, at high rotation speed, the motors might form a crystalline phase. Upon decreasing speed (by, *e.g.*, changing the ATP concentration), the lattice melts to form a

disordered (“high-temperature”) phase. In this paper, we describe this order phenomenon in detail and present some novel results characterizing the high-temperature phase. Finally, inspired by recent studies of the disease *situs inversus*, we discuss how an appropriate spatial arrangement of rotatory motors confined to a finite geometry can enhance left-right symmetry-breaking transport.

The remainder of this paper is organized as follows: First, we calculate the flow field of motor proteins embedded in a lipid membrane by discussing rotational monopoles and dipoles separately. In Section 3 we demonstrate that the interactions between the flow fields of the motors lead to an effective repulsion between them and we discuss the properties of the low-temperature crystalline phase. In Section 4 we analyze the high-temperature behavior of many motor systems. In particular, we discuss implications for situations which might be relevant for the pathology *situs inversus*. We conclude with a summary and an outlook.

2 Hydrodynamic flow field

We start by calculating the velocity field created by a single monopolar or dipolar motor. In the following, we assume the motors to be embedded in a flat manifold at $z = 0$ with a shear surface viscosity η_m . The manifold is surrounded by an incompressible solvent of density ρ_l which is either Newtonian or viscoelastic. The manifold contains N motors at position \mathbf{r}_i , where $\mathbf{r} \equiv (\mathbf{x}, z)$ denotes the position in 3-dimensional space and $\mathbf{x} \equiv (x_1, x_2)$ the position on the surface.

For the systems mentioned above flow occurs at low Reynolds number Re . Typical values for ATPase are $\omega \simeq 100\text{--}1000\text{ s}^{-1}$ for the angular velocity and $R \simeq 10\text{ nm}$ for its size [28,29]. For cilia $\omega \simeq 10\text{--}100\text{ s}^{-1}$ and $R \simeq 5\text{ }\mu\text{m}$ [7]. Thus, $Re \simeq 10^{-7}$ and $Re \simeq 10^{-3}$, respectively. For rotors driven by an external field $\omega \simeq 10\text{--}100\text{ s}^{-1}$ and $R \simeq 100\text{ }\mu\text{m}$ should be realizable. Then, $Re \simeq 10^{-1}\text{--}1$.

We first consider the simplest monopolar motor, a spinning sphere of radius R embedded into a surface with negligible surface viscosity ($\eta_m = 0$) surrounded by a Newtonian fluid with viscosity η . In the limit of small Reynolds numbers, the velocity field \mathbf{v} induced by a rotation with angular-velocity vector $\boldsymbol{\omega} = \omega \mathbf{e}_z$ is a solution of the Stokes equation. Due to rotational symmetry, the pressure p is constant [30] and the velocity \mathbf{v} is in the direction of $\mathbf{e}_\varphi \equiv \mathbf{e}_z \times \mathbf{r}/(r \sin \theta)$, where in spherical coordinates $\mathbf{r} = r(\sin \theta \cos \varphi, \sin \theta \sin \varphi, \cos \theta)$. Therefore,

$$\Delta \mathbf{v} = 0. \quad (1)$$

Since for an incompressible fluid $\text{div } \mathbf{v} = 0$, we write the velocity field as $\mathbf{v} = \text{rot } \mathbf{A}$, where \mathbf{A} is an axial vector. The ansatz $\mathbf{A} = f\boldsymbol{\omega}$ and equation (1) lead to $\Delta f = 0$ and $\nabla f = (2ar - \frac{b}{r^2}) \mathbf{e}_r$, where $\mathbf{e}_r \equiv \mathbf{r}/r$. The boundary conditions are $v \rightarrow 0$ as $r \rightarrow \infty$ and $\mathbf{v}(r = R) = \boldsymbol{\omega} \times \mathbf{r}$. Thus, one obtains for the velocity field

$$\mathbf{v} = \frac{R^3}{r^3} \boldsymbol{\omega} \times \mathbf{r}. \quad (2)$$

In the simplest description, rotational dipoles on such a surface can be thought of as being built up by two spheres separated by a distance d with angular-velocity vectors $-\boldsymbol{\omega}$ and $\boldsymbol{\omega}$. If the two spheres are located at $\mathbf{r}_1 = (0, z = 0)$ and $\mathbf{r}_2 = (0, z = d)$, then the velocity field at \mathbf{r} (for $r \gg d$) is at first order in d given by

$$\mathbf{v}(\mathbf{r}) = \frac{3R^3 dz}{r^5} \boldsymbol{\omega} \times \mathbf{r}. \quad (3)$$

Again, the direction of the flow field is along the orthoradial vector \mathbf{e}_φ .

Due to the rotational symmetry, the Stokes equation (1) and therefore the flow field (2) are independent of the viscosity η . It should be emphasized that this is a direct consequence of our assumption that the motors work at constant angular velocity ω . Since at low Reynolds numbers the transient oscillations (which occur upon momentum injection) can be neglected, the fluid behaves effectively as a non-viscous one.

However, the viscosity η sets the scale for the relevant forces. To make this point clearer, we calculate the viscous torque exerted by the fluid on one sphere. The only non-vanishing component of the corresponding viscous stress tensor is given by $\sigma_{r\varphi} = \eta \left(\frac{\partial v}{\partial r} - \frac{v}{r} \right) \Big|_{r=R} = -3\eta\omega \sin\theta$. Thus, the total torque is given by

$$\tau = \int_0^{2\pi} d\varphi \int_0^\pi d\theta R^3 \sin^2\theta \sigma_{r\varphi} = -8\pi\eta R^3 \omega. \quad (4)$$

The applied torque has the direction of the rotation vector $\boldsymbol{\omega}$, $\boldsymbol{\tau} = \frac{\tau}{\omega} \boldsymbol{\omega}$. The velocity field can be written as a function of the torque as

$$\mathbf{v} = -\frac{3\tau dz x}{8\pi\eta r^5} \mathbf{e}_\varphi. \quad (5)$$

For a more realistic description of biologically relevant dipolar motors such as ATPase, one must take into account the membrane viscosity $\eta_m \neq 0$ so that the viscosities seen by the two rotating portions of the motor are different. Cilia are linked to the cytoskeleton. This situation can be captured by the limit of large membrane viscosity where the support of the motor becomes solid-like.

For simplicity, we assume that the motor consists of two circular disks with radii R at $z = d$ and $z = 0$. This should yield a realistic description for the flow field far away from ATPase ($d/z \ll 1$) [28, 29]. Here, we concentrate on this macroscopic description. In Appendix A we sketch how the motor ATPase is described by an Onsager theory.

We describe the flow field of one motor as being created by a set of localized forces in the fluid. By introducing a discrete distribution of p force centers at the edge of the disks, the force density associated with the rotational motion is given by

$$\mathbf{f}(\mathbf{r}) = -\frac{\tau}{R^2 \omega p} \sum_{j=1}^p \boldsymbol{\omega} \times \mathbf{x} \delta(\mathbf{x} - \mathbf{x}_j) [\delta(z - d) - \delta(z)], \quad (6)$$

with $\mathbf{x}_j = R(\cos\theta_j, \sin\theta_j)$ and $\theta_j = 2\pi j/p$.

In-plane Fourier transformation for $p \gg 1$ and $qR \ll 1$ yields

$$\begin{aligned} \mathbf{f}(\mathbf{q}, z) &= -\frac{\tau}{R^2 \omega p} \sum_{j=1}^p i\mathbf{q} \cdot \mathbf{x}_j \boldsymbol{\omega} \times \mathbf{x}_j [\delta(z - d) - \delta(z)] = \\ &= -\frac{1}{2} \frac{\tau}{\omega} i\boldsymbol{\omega} \times \mathbf{q} [\delta(z - d) - \delta(z)] \equiv \\ &= -\mathbf{f}_0(\mathbf{q}) [\delta(z - d) - \delta(z)]. \end{aligned} \quad (7)$$

A motor that is not subject to an external field cannot inject kinetic momentum into the fluid and the total torque associated with the force distribution therefore vanishes as one can check. The two parts of the motor exert opposite torques and from a mechanical point of view, a dipolar motor corresponds to a torque dipole.

As shown in Appendix B the velocity field can be calculated by solving the coupled Stokes equation for the external fluid and for the membrane in the presence of this force field by using Fourier components in the plane of the membrane. The velocity is as above parallel to the plane of the membrane and in the orthoradial direction. Transforming back to \mathbf{x} -space one has in polar coordinates

$$\mathbf{v}(\mathbf{r}) = v_\varphi \mathbf{e}_\varphi = -\mathbf{e}_\varphi \frac{\tau d}{8\pi\eta} \int_0^\infty dq q^2 G(q, l) e^{-q|z|} J_1(qx). \quad (8)$$

Here, J_ν denotes the Bessel functions of the first kind [31] and the propagator is given by

$$G(q, l) \equiv \begin{cases} \frac{1}{1 + ql} & \text{for } z < 0, \\ \frac{1}{1 + ql} - 2 & \text{for } z > 0. \end{cases} \quad (9)$$

The length $l = \frac{\eta_m}{2\eta}$ characterizes the surface viscosity of the membrane. In principle, the scale of l is set by the membrane thickness but experimentally it is found to be at least 100 times larger [32].

For $l = 0$, equation (8) leads to

$$v_\varphi = -\frac{3\tau d}{8\pi\eta} \frac{zx}{(z^2 + x^2)^{5/2}}, \quad (10)$$

with $\mathbf{v}(\mathbf{r}) = v_\varphi \mathbf{e}_\varphi$ everywhere (except for the region $0 < z < d$), in agreement with equation (5). In the case of cilia, for $l = \infty$ one has

$$\mathbf{v}(\mathbf{r}) = \begin{cases} 0 & \text{for } z < 0, \\ 2v_\varphi \mathbf{e}_\varphi & \text{for } z > 0. \end{cases} \quad (11)$$

Note that, in the case of a solid-like membrane the flow field does not penetrate through the membrane.

Similarly, one finds (as also shown in App. B) for the velocity field created by a monopolar motor embedded in a membrane:

$$\mathbf{v}(\mathbf{r}) = -\mathbf{e}_\varphi \frac{\tau}{8\pi\eta} \int_0^\infty dq q G^{(m)}(q, l) e^{-q|z|} J_1(qx), \quad (12)$$

where

$$G^{(m)}(q, l) = \frac{1}{1 + ql} \quad (13)$$

for all values of z .

Equation (12) reduces to equation (2) for $l = 0$. For large l one finds

$$\mathbf{v}(\mathbf{r}) = e_\varphi \frac{xR^3\omega}{lr(z+r)}. \quad (14)$$

Note that membrane-embedded monopolar and dipolar motors can be investigated simultaneously by writing

$$\mathbf{v}(\mathbf{r}) = -e_\varphi \frac{\tau}{8\pi\eta} \int_0^\infty dq q^2 hG(q, l) e^{-ql|z|} J_1(qx). \quad (15)$$

Here, $G(q, l) \equiv (1 + ql)^{-1} - \alpha 2\theta(z)$ with the Heaviside function $\theta(z)$. Then, for $h = d$ and $\alpha = 1$ the last equation reduces to equation (8), whereas for $h = 1/q$ and $\alpha = 0$ one obtains equation (12).

Finally, we give some estimates for the order of magnitude of the flow field. For monopoles (on surfaces with $\eta_m = 0$) with radii in the micrometer range and $\omega \simeq 100 \text{ s}^{-1}$, one has $v \simeq 100 \mu\text{m/s}$ in the vicinity of the motor. For ATPase, however, one has $v \approx d\omega \simeq 1 \mu\text{m/s}$ and for cilia $v \simeq 100 \mu\text{m/s}$.

3 Interaction between motors and behavior at high rotation speed

We now consider an ensemble of N motors confined to a flat surface and discuss the effect of the hydrodynamic interactions between them. We first consider the case where surface viscosity is negligible.

3.1 Monopolar motors on manifolds with $\eta_m = 0$

Since Stoke's equation (1) is linear, the flow field created by an assembly of N motors at positions \mathbf{x}_i reads

$$\mathbf{v}_t(\mathbf{r}) = R^3 \int d^2x' \rho(\mathbf{x}') \boldsymbol{\omega} \times \frac{\mathbf{r} - \mathbf{r}'}{|\mathbf{r} - \mathbf{r}'|^3}, \quad (16)$$

where $\rho(\mathbf{x}) = \sum_{i=1}^N \delta(\mathbf{x} - \mathbf{x}_i)$ is the two-dimensional density of motors.

This expression is formally equivalent to the Biot and Savart law of classical electrodynamics (see, *e.g.*, [33]). Here, \mathbf{v} plays the role of the magnetic field \mathbf{B} which is induced by a current $\mathbf{j}(\mathbf{x}, z) = \rho(\mathbf{x})\boldsymbol{\omega}\delta(z)$. Furthermore, vortex lines in rotating superfluid helium create the same velocity field [34]. Monopolar motors can be interpreted as vortex points in two dimensions of strength $\kappa = \oint \mathbf{dl} \cdot \mathbf{v} = 2\pi\omega R^2$.

We assume that each motor follows the local (planar) flow in the confining surface. Thus, a motor at position \mathbf{r}_0 has velocity $\mathbf{v}_t(\mathbf{r}_0)$. For a discrete set of motors in an external field one finds

$$\frac{d\mathbf{x}_i}{dt} = R^3 \sum_{j \neq i} \frac{\boldsymbol{\omega} \times (\mathbf{x}_i - \mathbf{x}_j)}{|\mathbf{x}_i - \mathbf{x}_j|^3} + \mathcal{O}\left(\frac{R^6\omega}{|\mathbf{x}_i - \mathbf{x}_j|^5}\right). \quad (17)$$

Here, the neglected terms arise from the fact that the flow field $\mathbf{v}(\mathbf{x}_j)$ of motor j alters the no-slip boundary condition for motor i at position \mathbf{x}_i . However, these corrections are small for low densities, *i.e.* for $|\mathbf{x}_i - \mathbf{x}_j| \gg R$.

It is interesting to note that these coupled equations of motion have the structure of a Hamiltonian system (*cf.*, *e.g.*, [35]) with Hamilton function $H = H(p_1, \dots, p_N, q_1, \dots, q_N)$, where for $\mathbf{x}_i = (x_{i1}, x_{i2})$ one has $p_i \equiv x_{i1}$ and $q_i \equiv x_{i2}$ and

$$H(p_1, \dots, p_N, q_1, \dots, q_N) = -\omega R^3 \times \sum_{i,j} \frac{1}{|(p_i - p_j)^2 + (q_i - q_j)^2|^{1/2}}. \quad (18)$$

Writing the equations of motion with the help of a Hamilton function has the advantage that the symmetries of the system become evident. For example, since H is a constant of motion (*i.e.* $dH/dt = 0$), motors cannot collide. In particular, at all times $t > 0$ the minimal distance between motors is bound (from below) by the initial motor distribution at $t = 0$.

To investigate the hydrodynamic interactions between the motors, it is useful to introduce the pseudo-energy

$$E_{\text{kin}} = \pi\rho_l R^6 \omega^2 \sum_{j \neq i} \frac{1}{|\mathbf{x}_i - \mathbf{x}_j|} = \pi\rho_l R^6 \omega^2 \int d^2x \int d^2x' \frac{\rho(\mathbf{x})\rho(\mathbf{x}')}{|\mathbf{x} - \mathbf{x}'|}, \quad (19)$$

where ρ_l is the fluid density. A direct calculation using expression (16) of the velocity created by the assembly of motors shows that $E_{\text{kin}} = \frac{1}{2}\rho_l \int d^3x \mathbf{v}_t^2(\mathbf{x})$ is the total kinetic energy of the fluid. The equation of motion (17) of a motor can then be rewritten as

$$2\pi\rho_l R^3 \frac{d\mathbf{x}_i}{dt} \times \boldsymbol{\omega} = -\frac{\delta E_{\text{kin}}}{\delta \mathbf{x}_i}. \quad (20)$$

The assembly of motors therefore reaches a steady state if the effective kinetic energy E_{kin} is extremal. Note that in equation (19) ρ_l has been introduced artificially and there are no inertial effects in this force balance. The effective hydrodynamic interactions between motors are thus long range and repulsive and decay as $1/x$ [36]. In the absence of thermal fluctuations we thus predict that in a steady state, the motors should form a Wigner-like "crystal" and order on a triangular lattice. We refer to this ordered state as a crystal even though it is not evident that it indeed exhibits quasi-long-ranged translational order since dislocation pairs are free to separate to arbitrary (but finite) distances.

Thus, even though we are considering a viscous system the kinetic energy provides the relevant functional for the equations of motion. This is in agreement with the equivalent electrodynamic problem, where the energy density \mathcal{E}_{em} is given by the electromagnetic field tensor F_{ij} , *i.e.*

$$\mathcal{E}_{\text{em}} = \frac{1}{16\pi c} F_{ij} F^{ij} \equiv \frac{1}{16\pi c} (\partial_i A_j - \partial_j A_i)(\partial^i A^j - \partial^j A^i) = \frac{1}{16\pi c} B^2, \quad (21)$$

where A_i are the components of the vector potential and where for the static problem $i, j = 1, 2, 3$. Since the magnetic field \mathbf{B} corresponds to $\mathbf{v}_t(\mathbf{r})$, the electromagnetic energy corresponds to the effective kinetic energy E_{kin} of the system. Thus, even for systems with small (but finite) Reynolds number the kinetic energy is the only candidate for a functional for the equations of motion. However, one should note that the kinetic energy is only a well-defined quantity because the motors are assumed to be rotating at constant ω . Finally, there is a subtle difference between our problem and magnetostatic problems, since the current $\mathbf{j} = \rho\boldsymbol{\omega}$ is not necessarily divergence-free, *i.e.* in general $\frac{\partial \rho(\mathbf{x})}{\partial t} + \text{div}(\rho(\mathbf{x})\boldsymbol{\omega}) \neq 0$.

This “energetic” argument does not prove that a steady state exists and that a triangular lattice of motors is stable even in the absence of fluctuations. To discuss the stability of the triangular lattice, we consider a slightly disturbed lattice where motor i has been displaced from its equilibrium position $\mathbf{R}_i = \mathbf{R}_i^{(0)} + \delta\mathbf{R}(t)$. The equation of motion of the displaced motor is

$$\begin{aligned} \frac{d}{dt}\delta\mathbf{R}(t) &= R^3 \sum_{\substack{j \\ j \neq i}} \boldsymbol{\omega} \times \frac{\mathbf{R}_i^{(0)} + \delta\mathbf{R} - \mathbf{R}_j^{(0)}}{|\mathbf{R}_i^{(0)} + \delta\mathbf{R} - \mathbf{R}_j^{(0)}|^3} = \\ &= -3R^3 \sum_{m=1}^{\infty} \boldsymbol{\omega} \times \frac{1}{m^3 a^3} \delta\mathbf{R} + \mathcal{O}(\delta R)^2, \end{aligned} \quad (22)$$

where a is the lattice constant. For the last equation we have used that for a triangular lattice

$$\sum_{k=1}^6 \frac{\mathbf{a}_k}{a^2} \delta\mathbf{R} \cdot \mathbf{a}_k = 3\delta\mathbf{R}. \quad (23)$$

Here,

$$\mathbf{a}_1 = a\mathbf{e}_y, \quad \mathbf{a}_2 = a\frac{\sqrt{3}}{2}\mathbf{e}_x + \frac{a}{2}\mathbf{e}_y, \quad \mathbf{a}_3 = a\frac{\sqrt{3}}{2}\mathbf{e}_x - \frac{a}{2}\mathbf{e}_y, \quad (24)$$

and

$$\mathbf{a}_1 = -\mathbf{a}_4, \quad \mathbf{a}_2 = -\mathbf{a}_5, \quad \mathbf{a}_3 = -\mathbf{a}_6. \quad (25)$$

The equation of motion (22) describes a rotation of the motor around its initial position with rotational vector $\tilde{\boldsymbol{\omega}} = -\tilde{\omega}\mathbf{e}_z$ and constant frequency $\tilde{\omega}$. Thus,

$$\delta\mathbf{R} = r(t) \begin{pmatrix} \cos \tilde{\omega}t \\ -\sin \tilde{\omega}t \\ 0 \end{pmatrix}, \quad (26)$$

and equation (22) yields

$$\tilde{\omega} = 3\omega \sum_{m=1}^{\infty} \frac{R^3}{m^3 a^3} = 3\zeta(3)\omega \frac{R^3}{a^3}, \quad (27)$$

where $\zeta(x)$ is Riemann’s zeta-function [31].

At the level of linear hydrodynamics that we have used so far (we used the Stokes equation of motion and not the

full Navier-Stokes equation), the triangular lattice of motors is thus only marginally stable. A full stability analysis requires non-linear hydrodynamics. This goes beyond the scope of this work and we give only a qualitative argument. It is shown in references [24, 25] that the first-order inertial correction to the Stokes equation generates a force acting on the displaced motor. This force is the Magnus force $\mathbf{F}_M = -2\pi\rho_l R^3 r \tilde{\omega} \mathbf{e}_\varphi \times \boldsymbol{\omega}$, where the velocity is the rotation velocity at an angular velocity $\tilde{\omega}$ around the equilibrium lattice site. The Magnus force on the displaced motor points towards the equilibrium position and thus stabilizes the lattice.

In order to estimate the relaxation towards the equilibrium position, we parameterize the motor position by equation (26) and we calculate the radius $r(t)$ by balancing the Magnus force \mathbf{F}_M with a viscous drag force with a Stokes friction of order $6\pi\eta R$:

$$6\pi\eta R \frac{dr}{dt} = -2\pi\rho_l \omega r(t) \tilde{\omega} R^3. \quad (28)$$

Thus, $r(t)$ decays exponentially with a relaxation time $1/t_R \sim \rho_l \omega \tilde{\omega} R^2 / (3\eta) \sim \zeta(3)\rho_l \omega^2 R^5 / (\eta a^3)$.

The critical frequency ω_c at which the crystal melts can be obtained by comparing the relaxation time t_R with a characteristic time of thermal fluctuations given by the diffusion time over a lattice constant $t_D = a^2/D = 6\pi\eta R a^2 / kT$. Melting occurs for $t_R \simeq t_D$ or at frequencies $\omega < \omega_c$ with

$$\omega_c^2 \simeq \frac{akT}{6\zeta(3)\pi\rho_l R^6}. \quad (29)$$

The Lindeman criterion (where $kT = a^2 \partial^2 U(\omega = \omega_c) / \partial x^2$, with $\partial U / \partial x = F_M$) yields the same critical frequency ω_c . However, for the dynamical situation here, the phenomenological melting criterion based on the comparison of the two time scales is more appropriate. More systematic approaches will have to consider collective excitations, *i.e.* the unbinding of topological defects, which will yield a melting criterion similar to the one of Kosterlitz and Thouless for lattices in thermodynamic equilibrium [37]. We leave the investigation of this point for future work.

Equation (29) also shows that for Newtonian fluids crystallization is only experimentally observable if inertial effects are sufficiently strong. Since the relevant time scale t_v is set by diffusion of vorticity, where $t_v = \rho R^2 / \eta$, the above melting criterion can be written as

$$\omega_c^2 \simeq \frac{akT}{6\zeta(3)\pi t_v R^4 \eta}. \quad (30)$$

If inertial effects are negligible, crystallization does not occur in ideal Newtonian fluids where no viscous analog of the Magnus force exists [38]: a viscous Magnus force \mathbf{F}_M^V would have to break time-reversal symmetry and in the absence of additional time scales any combination of $\mathbf{v} \times \boldsymbol{\omega}$ is symmetric under time-reversal. In real (viscoelastic) fluids, such an additional time scale is present given by the microscopic relaxation time t_m . Then [39],

$$\mathbf{F}_M^V = 6\pi\eta R t_m \mathbf{v} \times \boldsymbol{\omega}. \quad (31)$$

For the biological materials considered here, viscoelastic effects dominate over inertia and one can replace t_v by t_m in equation (30). For a crystal of rotating objects with the size of a few nanometers one has $\omega_c \simeq t_m^{-1}$ (at room temperature).

3.2 Monopolar and dipolar motors on membranes

We now discuss dipolar motors and then show how these results can be generalized to monopolar motors embedded in a membrane with $\eta_m \neq 0$.

To describe the motion of dipolar motors in a Newtonian solvent, we introduce the bulk friction $\zeta \sim 6\pi\eta R$ for the fluid part of the motor and the membrane friction for the membrane-embedded part $\zeta_m \sim 6\pi\eta l$. The actual velocity \mathbf{v} of the motor is given by the balance of the friction forces on the motor, *i.e.*

$$\zeta(\mathbf{v} - \mathbf{v}_t(d)) + \zeta_m(\mathbf{v} - \mathbf{v}_t(0)) = \mathbf{0}, \quad (32)$$

where the velocities above the membrane $\mathbf{v}_t(d)$ and in the membrane $\mathbf{v}_t(0)$ for one motor are given by equation (8) in the limits where $z \rightarrow 0^+$ and $z \rightarrow 0^-$, respectively. Summing over the velocity fields created by all motors, we find

$$\mathbf{v}_t(\mathbf{x}) = \frac{\tau d}{4\eta\omega} \int d^2x' G(\mathbf{x} - \mathbf{x}') \boldsymbol{\omega} \times \nabla \rho(\mathbf{x}'). \quad (33)$$

The kernel G is obtained by inverse Fourier transformation of $G(q)$ given by equation (9) (for $z < 0$)

$$G(x) = \frac{1}{2\pi l x} \left[1 - \frac{\pi x}{2l} [H_0(x/l) - N_0(x/l)] \right], \quad (34)$$

where H_0 is the Struve function and N_0 the Neumann function defined in reference [31]. If $x \ll l$, $G(x) = 1/(2\pi l x)$ and if $x \gg l$, $G(x) = l/(2\pi x^3)$. The velocity of a motor vanishes both for $l = 0$ because of symmetry and for $l \rightarrow \infty$, since then the membrane viscosity is infinite and no motion is possible.

The interactions between the motors are studied in a similar way as for non-dipolar motors. We introduce the pseudo-energy

$$E = 2\pi^2 \rho_l R^6 \omega^2 d \int d^2x \int d^2x' \rho(\mathbf{x}) \rho(\mathbf{x}') G(\mathbf{x} - \mathbf{x}'). \quad (35)$$

Then, the equation of motion of a motor is given by equation (20) with E replacing E_{kin} (the prefactor has been chosen in such a way that Eq. (20) remains valid). A steady-state distribution of the motors therefore corresponds to an extremum of the energy E . The energy E corresponds to the kinetic energy of the fluid only for $G(x) = 1/x$. The hydrodynamic interactions between motors are again long range and repulsive and the dipolar motors tend to arrange on a triangular lattice. The stability of the lattice can be studied as above. At the level of the Stokes equation the lattice is marginally stable and it can only be stabilized by the inertial Magnus force \mathbf{F}_M or its viscous analog \mathbf{F}_M^v .

Since for motors in a membrane the viscous friction is in general dominated by the membrane friction $\zeta_m \sim \eta_m \sim \eta l$ the critical frequency is $\omega_c \sim [a^3 kT / (t_v R^4 \eta l d)]^{1/2}$ at low densities ($a \gg l$) and $\omega_c \sim [a l kT / (t_v R^4 \eta d)]^{1/2}$ at high densities ($a \ll l$). Again, for viscoelastic fluids ω_c can be obtained by replacing t_v by t_m in these formulas. All these results can be easily generalized to monopoles in membranes (by using the correspondence $d = 1/q$ and $\alpha = 0$).

Upon inserting for the lattice constant $a \simeq 10R$ (a value which could be achieved experimentally) we find an extremely high ω_c ($\omega_c \simeq 10^{16} \text{ s}^{-1}$) for nanometer scale motors in a Newtonian solvent. However, for viscoelastic solvents the hydrodynamic interactions are much stronger and crystallization occurs at experimentally achievable frequencies. These crystallization effects might even be large enough to be relevant for real biological systems (such as, *e.g.*, ATPsynthase in mitochondria) provided $t_m \simeq \omega_c^{-1}$. Ordering phenomena can probably be observed by attaching actin filaments to the F_1 -portion [29] or by using motors of the size of cilia. For monopolar macroscopic motors, ordered structures have been observed [24, 25].

4 Disordered assembly of motors on a membrane

In most instances (at sufficiently low rotation speed ω), the hydrodynamic interactions between motors are small and the motors form a disordered gas on the membrane. We discuss in this section three properties of a disordered assembly of motors on a membrane: i) active diffusion induced by the rotation of the motors, ii) coupling between the membrane fluctuations and the motor velocity field, and iii) the velocity field induced by a non-homogeneous distribution of motors. The last scenario could be relevant for cilia-generated flow and the analysis of Hirokawa's experiments on the disease *situs inversus*.

4.1 Active diffusion in the membrane

In the membrane, the fluctuations of the local density of motors induce local fluctuations in the velocity field. The convection by these velocity fluctuations creates an active diffusion of the motors. The active contribution to the diffusion constant is proportional to the time correlation function of the velocity fluctuations:

$$\delta D = \frac{1}{2} \int_0^\infty dt \langle \mathbf{v}(\mathbf{x}, t) \mathbf{v}(\mathbf{x}, 0) \rangle. \quad (36)$$

By using the relationship (33) between density and velocity of the dipolar motors, one can express this contribution in terms of the density correlation function

$$\begin{aligned} \delta D &= \frac{1}{2(2\pi)^4} \int d^2q \int d^2q' \int_0^\infty dt \langle \rho(\mathbf{q}, t) \rho(\mathbf{q}', 0) \rangle \\ &\times \left(\frac{\tau d}{4\eta} \right)^2 G(q') G(q) (\mathbf{q}' \cdot \mathbf{q}). \end{aligned} \quad (37)$$

If the active diffusion is treated as a perturbation, the motors can in a first approximation be described as an ideal gas and the density correlation function is $\langle \rho(\mathbf{q}, t) \rho(\mathbf{q}', 0) \rangle = 4\pi^2 \delta(\mathbf{q} - \mathbf{q}') \rho \exp(-D_m q^2 t)$, where ρ is the average density in the membrane and $D_m \sim (6\pi\eta l)^{-1}$ the collective two-dimensional diffusion constant of the motors in the membrane. This leads to an active contribution to the diffusion constant,

$$\frac{\delta D}{D_m} = \frac{\rho}{4\pi D_m^2} \left(\frac{\tau d}{4\eta l} \right)^2 \log(1 + q_{\max} l) + \mathcal{O}\left(\frac{\delta D^2}{D_m^2}\right) = \frac{9\pi\rho d^2}{16} \left(\frac{\tau}{kT} \right)^2 + \mathcal{O}\left(\frac{\delta D^2}{D_m^2}\right), \quad (38)$$

since for small densities ρ one has $q_{\max} < 1/l$. Equation (38) holds for arbitrary rotation speeds $\omega < \omega_c$.

The active contribution to the diffusion constant is small for bare ATPase (where $\tau \simeq 0.01kT$) but it can become important for actin-labeled ATPase ($\tau \simeq 10kT$) and larger objects of the size of cilia. Note also that in linear hydrodynamics and if the coupling to membrane fluctuations (cf. the subsequent section) is ignored, the friction on a motor ζ_m is not changed by the rotation and that the active contribution to the diffusion constant could be characterized by an effective temperature defined via the fluctuation-dissipation theorem by $D_m + \delta D = T_{\text{eff}}/\zeta_m$.

In a similar fashion the velocity-velocity correlation function can be calculated. Here, one finds

$$\langle v_\alpha(\mathbf{x}, t) v_\beta(\mathbf{x}, 0) \rangle = \delta_{\alpha\beta} |\varepsilon^{\alpha\gamma}| \frac{\rho}{4\pi^2} \left(\frac{\tau d}{4\eta} \right)^2 \times \int dq_1 dq_2 \frac{q_\gamma^2}{(1 + l\sqrt{q_1^2 + q_2^2})^2} \exp(-D_m t(q_1^2 + q_2^2)), \quad (39)$$

where $\delta_{\alpha\beta}$ is Kronecker's delta and $\varepsilon^{\alpha\beta}$ the Levi-Civita symbol. Thus, $\langle v_\alpha(\mathbf{x}, t) v_\alpha(\mathbf{x}, 0) \rangle \sim t^{-2}$ for large t and small l and $\langle v_\alpha(\mathbf{x}, t) v_\alpha(\mathbf{x}, 0) \rangle \sim t^{-1}$ for large t and large l .

4.2 Coupling between rotating motors and membrane fluctuations

So far, we have only considered flat membranes and ignored the coupling between the undulation fluctuations of the membrane and the rotating motors. The coupling has two effects: a) the flow created by the motors can perturb the membrane fluctuations as has been observed, *e.g.*, in experiments on membranes containing bacteriorhodopsin pumps [19]; and b) the undulations of the membranes also perturb the flow created by the motors.

In order to demonstrate this effect, we choose the Monge representation to parameterize the membrane. The position of the membrane at time t is given by $(x_1, x_2, h(x_1, x_2, t))$ and the normal vector to the surface by $\mathbf{n} = (-\partial_1 h, -\partial_2 h, 1)$. We assume that the motors remain normal to the membrane and that the flow created by a dipolar motor can be characterized as before

by torques exerted by the two parts of the motor with a direction normal to the membrane. In complete analogy with the analysis of Section 2, we calculate the density of localized forces in the fluid induced by the motors with an orientation that follows that of the membrane. If $\psi(\mathbf{r})$ denotes the three-dimensional density of motors, then the total force (per volume) at position \mathbf{r} exerted by all motors can be written as

$$\mathbf{F}(\mathbf{r}) = \frac{i\tau}{2} \int d^3 r' \int d^3 k \psi(\mathbf{r}') e^{i\mathbf{k} \cdot (\mathbf{r} - \mathbf{r}')} \mathbf{k} \times \mathbf{n}(\mathbf{r}'). \quad (40)$$

By defining the two-dimensional motor density $\psi(\mathbf{x}, z) = \rho(\mathbf{x}) \delta(z - h(\mathbf{x}))$, one obtains after Fourier transformation and an integration over z

$$\mathbf{F}(\mathbf{k}) = \frac{i\tau}{2} \int d^2 x \rho(\mathbf{x}) e^{iq_z h(\mathbf{x})} e^{-i\mathbf{q} \cdot \mathbf{x}} \mathbf{q} \times \mathbf{n}(\mathbf{x}), \quad (41)$$

where $\mathbf{k} = (\mathbf{q}, q_z)$. By expanding $\rho(\mathbf{x}) = \rho_0 + \delta\rho(\mathbf{x}) + \mathcal{O}(h^2)$, one obtains two contributions to the force distribution: i) a contribution linear in $\delta\rho(\mathbf{q})$ which is the force due to the motor density fluctuations on a flat membrane, and ii) a contribution due to the membrane fluctuations given by

$$\mathbf{F}(\mathbf{k}) = i2 \frac{\tau}{\omega} \rho_0 q_z h(\mathbf{q}) \mathbf{q} \times \boldsymbol{\omega} + \mathcal{O}(h^2), \quad (42)$$

where $h(\mathbf{q})$ is the Fourier transform of $h(\mathbf{x})$. Back-transformation to the spatial variable z then yields for the force distribution

$$\mathbf{F}(\mathbf{q}, z) = \frac{\tau}{\omega} \rho_0 h(\mathbf{q}) \delta'(z) \mathbf{q} \times \boldsymbol{\omega}. \quad (43)$$

Consequently, the flow field consists of two contributions $v_{\text{tot}} = v_t + v_m$, where v_t is the flow field caused by fluctuations in the density of motors (cf. Eq. (33)) and v_m is the flow field due to membrane fluctuations:

$$\mathbf{v}_m(\mathbf{q}, z) = \frac{i\tau d}{2\eta\omega} \boldsymbol{\omega} \times \mathbf{q} e^{-q|z|} G_m(q) \rho_0 q h(\mathbf{q}), \quad (44)$$

where the relevant kernel is $G_m(q, l) \equiv -1/(1 + ql)$. The essential result is that even in the presence of membrane fluctuations, the flow remains parallel to the average plane of the membrane. Thus, in lowest order the fluctuation spectrum of the membrane is not modified by the flow induced by the motors. However, the membrane fluctuations do influence the flow field on the membrane. Therefore, they will influence the distribution of motors and the active contribution to the in-plane diffusion constant of the motors $D_m + \delta D$ given by equation (38).

However, as detailed in Appendix A, ATPsynthase influences the hydrodynamics of the system in a twofold manner. On the one hand, it is a rotating motor that exerts a torque dipole. On the other, it is also a proton pump which exerts a local force quadrupole [40]. In the linear theory considered here, the two contributions to the flow decouple and can be simply added up. Then, only the proton pump has an effect on the membrane fluctuation quite similar to that of the bacteriorhodopsin studied in reference [20]. The coupling between the motor rotation and the membrane fluctuations only appears at non-linear order and is neglected here.

4.3 Non-homogeneous motor distribution

In this section, we discuss two situations where the in-plane distribution of motors is non-homogeneous. As the dynamics of the motors becomes chaotic in the high-temperature phase (*i.e.* for small ω), their motion might reach a stable attractor corresponding to arrangements with stationary but inhomogeneous motor density, *i.e.* arrangements which fulfill $\partial_t \rho(\mathbf{x}) = 0$ and therefore

$$\begin{aligned} \operatorname{div} \left(\rho(\mathbf{x}) \int d^2 x' \rho(\mathbf{x}') \mathbf{v}(\mathbf{x} - \mathbf{x}') \right) = \\ \nabla \rho(\mathbf{x}) \cdot \int d^2 x' \rho(\mathbf{x}') \mathbf{v}(\mathbf{x} - \mathbf{x}') = 0. \end{aligned} \quad (45)$$

An obvious candidate for a stationary configuration is a circle consisting of N uniformly distributed motors. As we show now, it is stable in the limit where the influence of thermal fluctuations on the position of the motors can be neglected.

We consider N motors homogeneously distributed on a circle $A = \{x \mid |x| \leq r_0\}$ with a density $\rho(\mathbf{x}) = \frac{N}{\pi r_0^2}$ for $\mathbf{x} \in A$, $\rho(\mathbf{x}) = 0$ otherwise. For monopolar motors in an external field, one finds by using Stoke's theorem for the in-plane velocity

$$\begin{aligned} \mathbf{v}_t(\mathbf{x}, z=0) = R^3 \int_A d^2 x' \rho(\mathbf{x}') \boldsymbol{\omega} \times \nabla \frac{1}{|\mathbf{x} - \mathbf{x}'|} = \\ \frac{R^3}{\pi r_0^2} N \omega \int_{\partial A} ds' \frac{1}{|\mathbf{x} - \mathbf{x}'|}, \end{aligned} \quad (46)$$

where ds' is a parameterization of the boundary ∂A of A and $\mathbf{x}' \in \partial A$. By symmetry, $\mathbf{v}_t(\mathbf{x}) = v_t(x) \mathbf{e}_\varphi$ and the in-plane velocity reads

$$\begin{aligned} v_t(x) = \frac{R^3 N \omega}{\pi r_0} \frac{2}{r_0 x (r_0 + x)} \\ \times \left[(r_0^2 + x^2) F\left(\frac{\pi}{2}, k\right) - (r_0 + x)^2 E\left(\frac{\pi}{2}, k\right) \right]. \end{aligned} \quad (47)$$

The elliptic functions $F(\varphi, k)$ and $E(\varphi, k)$ are defined in reference [31] and $k = \frac{2\sqrt{r_0 x}}{r_0 + x}$. Far away from the circle of motors, equation (47) reduces, for small $\varepsilon \equiv r_0/x \ll 1$, to

$$v_t(x) = R^3 N \omega \frac{1}{x^2} + \mathcal{O}(\varepsilon^2). \quad (48)$$

The far field of such a distribution is identical to that created by a single motor localized at the center of the circle rotating at a frequency $N\omega$. Inside the circle, for small $\tilde{\varepsilon} \equiv x/r_0 \ll 1$, one finds

$$v_t(x) = R^3 N \omega \frac{x}{r_0^3} + \mathcal{O}(\tilde{\varepsilon}^2). \quad (49)$$

Here, the velocity is very small for a large circular aggregate of motors and vanishes for $r_0/R \rightarrow \infty$. Close to the boundary of the circular aggregate, *i.e.* for $x = r_0(1 - \varepsilon)$ with $\varepsilon \ll 1$, it is necessary to introduce a cutoff $\alpha \sim$

R/r_0 in the angular integration, *i.e.* to replace $\int_0^{2\pi} d\varphi$ by $\int_0^{2\pi - 2\alpha}$, where $\alpha \equiv R/r_0$. Then

$$v_t(x) \sim -\frac{R^3 N \omega}{\pi r_0^2} (2 + \varepsilon) \log \alpha, \quad (50)$$

where in the last equation, contributions which stay finite in the limit $\alpha \rightarrow 0$ have been neglected. Thus, the circular arrangement rotates as a whole, with an x -dependent frequency. The bulk velocity field outside the membrane plane is simply obtained by replacing x by $\sqrt{x^2 + z^2}$ in the equations above.

Similar arguments hold for membrane-embedded motors. Here, we will just give the corresponding equations for dipolar motors, where

$$\begin{aligned} \mathbf{v}_t(\mathbf{x}, z) = \frac{\tau d}{4\eta\omega} \frac{1}{(2\pi)^2} \frac{N}{\pi r_0^2} \int_A d^2 x' \\ \times \int d^2 q e^{i\mathbf{q} \cdot (\mathbf{x} - \mathbf{x}')} i\boldsymbol{\omega} \times \mathbf{q} G(q, l) e^{-q|z|}. \end{aligned} \quad (51)$$

For simplicity, we only focus on the limits $l \rightarrow 0$ and $l \rightarrow \infty$. Then for $z > 0$, the last equation reduces to

$$\mathbf{v}_t(\mathbf{x}, z) = -\frac{\tau d}{8\eta} \frac{N\gamma}{r_0\pi^3} \frac{1}{\sqrt{r_0 x}} \frac{d}{dz} Q_{1/2} \left(\frac{x^2 + z^2 + r_0^2}{2r_0 x} \right), \quad (52)$$

where Q_ν is the associated Legendre function of order ν and the number γ is equal to 1 if $l = 0$ and to 2 if $l \rightarrow \infty$. The asymptotic behavior of equation (52) can be obtained directly from that given for a non-dipolar motor in an external field by replacing x by $\sqrt{x^2 + z^2}$ and by using that for $l = 0, \infty$ the flow field \mathbf{v}_d of the dipoles can be obtained from that of the monopoles \mathbf{v}_m by $\mathbf{v}_d(\mathbf{x}, z) = -3/2\gamma d \frac{\partial}{\partial z} \mathbf{v}_m(\mathbf{x}, z)$.

This circular configuration is only stable in the limit where thermal fluctuations are negligible: if a motor diffuses away from the boundary of the circular aggregate, it starts to rotate around the circle since there is no restoring force. The Magnus force caused by this circular motion that we discussed in the previous section then drives the motors even further away. Similar arguments apply to other stationary configurations such as stripes, ellipses, etc.

Our second example of a non-homogeneous distribution of motors is related to the pathology called *situs inversus*. It was pointed out in [7] that the velocity field created by the nodal cilia can lead to a (right-left) symmetry-breaking transport. It is obvious that a homogeneous arrangement of rotating motors which all have the same frequency cannot lead to the necessary symmetry breaking. Many cilia generate flow when homogeneously distributed on a surface by using beating patterns that are more complex than simple rotations. For simplicity, we concentrate here on inhomogeneous arrangements of rotating motors on the membrane.

To demonstrate that a gradient in density can produce a symmetry-breaking transport, we consider a distribution of dipoles on a stripe $A = \{(x_1, x_2) \mid 0 \leq x_1 \leq$

x_1^m and $-L/2 \leq x_2 \leq L/2$ with a density gradient in the x_1 -direction:

$$\rho(\mathbf{x}) = \rho_0 + \delta\rho(\mathbf{x}) \equiv \rho_0 + c(x_1^m - x_1)\theta(x_1^m - x_1)\theta(x_1), \quad (53)$$

where ρ_0 and c are constant and $\theta(x)$ is the Heaviside function. Then, the change in velocity due to the gradient is given by

$$\delta\mathbf{v}_t(\mathbf{r}) = \int d^2x' \delta\rho(\mathbf{x}')\mathbf{v}(\mathbf{r}'), \quad (54)$$

where $\mathbf{v}(\mathbf{r})$ is given by equation (8). For simplicity, we consider only the limits $l = 0$ and $l \rightarrow \infty$. The flow is in the x_2 -direction and for $z > 0$

$$\mathbf{v}_t(\mathbf{x}, z) = \mathbf{e}_{x_2} c \frac{\gamma\tau d}{8\pi\eta} \int_A d^2x' \frac{z}{(z^2 + |\mathbf{x} - \mathbf{x}'|^2)^{3/2}}. \quad (55)$$

The explicit calculation of the integral gives, for $L/x_1^m \gg 1$,

$$\mathbf{v}_t(\mathbf{x}, z) = \mathbf{e}_{x_2} c \frac{\gamma\tau d}{4\pi\eta} \arctan\left(\frac{zx_1^m}{z^2 + x_1^2 - x_1x_1^m}\right). \quad (56)$$

For mobile motors these density gradients are reduced by diffusion and therefore special boundary conditions are necessary to stabilize such configurations. Here, we discuss, as a special case, adsorbing boundary conditions.

We consider a collection of N mobile motors (which all rotate in the same direction) restricted to a non-symmetric triangular geometry which is motivated by the shape of the node in the mouse embryo. The boundary of this region is assumed to consist of adsorbing sites. Thus, motors which touch these sites stay there but they continue to rotate. Under these conditions, it is possible that density gradients build up if the motors follow the local flow.

To demonstrate this, we have numerically integrated equation (17) by starting from a homogeneous arrangement of motors. We then find that after some relaxation time all motors stick to the boundary and that they build up a flow field which enhances the symmetry-breaking transport. Note that, for the homogeneous distribution, left-right symmetry is already broken but the associated transport is weak since for finite lattices only the motors close to the boundaries contribute. However, homogeneous arrangements restricted to a *finite* geometry are unstable and the symmetry-breaking transport is enhanced in the final (stable) configuration.

Figure 1 shows two examples of a final configuration obtained by this procedure where all $N = 36$ motors stick to the boundary. The two triangles shown have lower angles $\alpha = 80$ deg and $\alpha = 20$ deg. In both cases, we find a flow field which has a non-vanishing component in the $(-x_1)$ -direction, implying thus that the symmetry-breaking transport goes from right to left.

For nodal cilia similar mechanisms might be relevant. Although it is hard to imagine that cilia or the cells they are attached to are mobile, the interactions between the cilia and the flow field could still build up density gradients. For example, it can be imagined that the flow bends cilia or generates stresses on the cells and thus locally influences the rotatory movement of the cilia and alters the flow pattern.

5 Summary and outlook

We have studied the properties of rotating motors in flexible liquid membranes. Our study is motivated by biological systems where active processes drive rotatory motion in membranes and generate hydrodynamic flow. The most prominent examples of systems for which the discussed physical mechanisms could be relevant are ATPsynthase molecules and rotating cilia in the nodal region of mammalian embryos. ATPsynthase produce ATP molecules from a proton gradient in mitochondria. During this process, they rotate rapidly in the membrane and represent a rotation dipole. Nodal cilia generate hydrodynamic flow and are involved in left-right symmetry breaking. In all cases, the rotating motors act as small microvortices and induce flow in the water surrounding the membrane. As an important finding, we show that even when the shape fluctuations of the membranes are taken into account, the flow induced by the motor rotation is parallel to the average plane of the membrane. Therefore, the fluctuation spectrum of the membrane is, to linear order in the membrane deformations, not affected by the rotation of the motors. This result is obtained by using a linear hydrodynamic theory and by assuming that the rotation axis of the motors is always parallel to the local membrane normal. Fluctuations in the orientation of the motors around the normal would couple to the membrane fluctuations. However, we believe that this effect is small. Non-linear hydrodynamic couplings could also lead to a change in the membrane undulation spectrum. In this case, one would have to identify the relevant non-linear couplings and to introduce them in the hydrodynamic equations. ATPsynthase motors act both as rotating motors and as proton pumps. The proton pump activity is coupled to the membrane undulations as in the case of bacteriorhodopsin pumps that has been studied both theoretically and experimentally. However, if non-linear hydrodynamic interactions are important, the rotational and the translational motion induced by ATPsynthase are coupled and cannot be simply added.

The hydrodynamic flow in the average plane of the membrane can affect the distribution of motors. This flow is driven by motor density gradients and by membrane fluctuations. We have discussed both the possible crystallization of the motors due to hydrodynamic interactions and the active diffusion of the motors in the membrane plane. For small motors of the size of ATPsynthase in Newtonian fluids all these effects are small. This is related to the fact that with the experimentally available numbers the torque τ exerted by each part of the motor on the fluid is much smaller than thermal excitations with energy of order kT . However, larger and observable effects will be obtained by attaching actin filaments to the rotor of the motor as done in reference [29] or in viscoelastic solvents where the hydrodynamic interactions are much stronger. Then, a Wigner-like crystallization is predicted similar to that observed with rotating discs driven by magnetic fields in reference [24]. For ATPsynthase under biological conditions, the surrounding solvent typically contains polymers with relaxation times in the range $t_m = 10^{-1}$ –100 s corresponding to $\omega_c \simeq 0.01$ –10 s^{-1} . For motors in a Newtonian

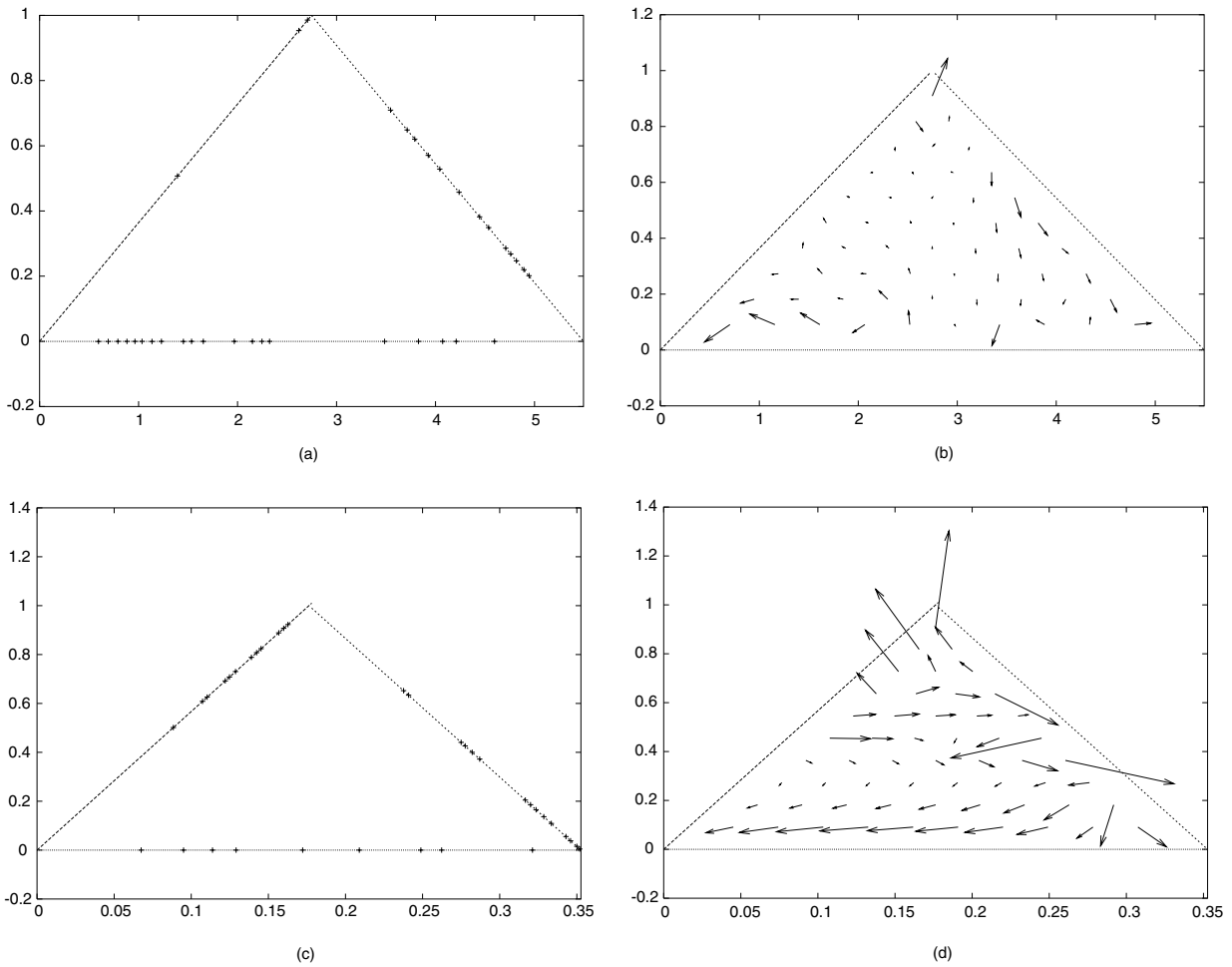


Fig. 1. System of motors confined to a triangular geometry with adsorbing sites on the boundaries. Starting from a homogeneous arrangement of motors, we have numerically integrated the coupled equations of motions until all motors have been adsorbed. (a) and (c) show the final configuration for triangles with lower angles $\alpha = 80$ deg and $\alpha = 20$ deg, respectively. (b) and (d) show the corresponding velocity fields on the triangle. Here, the velocity has units $\omega\sqrt{A}$, where A is the area of the triangle. In both cases, left-right symmetry is broken which is more pronounced for the lower geometry (see (d)), in agreement with the experimental findings [7].

fluid to which actin filaments of length $R \simeq 2 \mu\text{m}$ are attached, the transition should occur for $\omega_c = 100 \text{ s}^{-1}$, provided that $a \simeq 10 \mu\text{m}$.

The origin of the pathology *situs inversus* has been tracked down in reference [7] to the absence of flow in the node region of mouse embryos; the flow from right to left in the normal embryo is generated by a rotating motion of the cilia. Such a flow cannot exist for cilia with a rotationally invariant beating pattern when both the rotation speed (or rather the torque exerted by the motors on the fluid) and the density of motors are uniform in space. Having no indication concerning the heterogeneity of the rotation, we have performed calculations showing how a density gradient can enhance a symmetry-breaking flow and how it could originate from an initially uniform distribution of motors. Complementary hydrodynamic experiments would certainly be necessary for a better understanding of this problem. However, for the typical density of cilia in the nodal region of mice, hydrodynamic interac-

tions would be strong enough to yield a critical frequency $\omega_c \simeq 10 \text{ s}^{-1}$ (for $R \simeq 5 \mu\text{m}$).

Our approach can be extended in several ways. For example, one could consider collections of motors which can rotate in opposite directions. In fact, such mixtures might be relevant for chiral motors confined to non-viscous manifolds (where the motors can have two orientations). The phase diagram of systems with N_+ motors with rotational vector ω and N_- motors with rotational vector $-\omega$ is more complex than that for homogeneous collections. For high rotational speeds ω , two motors with opposite spin will form a bound pair moving freely in the system. However, in a first approximation our predictions presented here will remain valid and for high enough ω a crystal forms which now melts for $\omega < \omega_c^* \sim (a^*)^{1/2}$ with $a^* = a/|N_+ - N_-|^{1/2}$. Additionally, a liquid-to-gas transition takes place at a critical rotation speed $\omega_c^{\text{lg}} \simeq \omega_c^*$. Note that the case $N_+ = N_-$ is special since here no freezing transition takes place. One rather has a liquid

(vapor) phase with complicated interactions. Even more complex situations can occur in experimental realizations of membrane-embedded dipolar motors where the orientation of motors is difficult to control. Here, one can have mixtures of motors with rotational vectors ω_1 and $\omega_2 \neq \omega_1$ (depending on their orientation and the pH gradient across the membrane).

We thank J. Kurchan, U. Seifert and K. Sekimoto for useful discussions. P.L. acknowledges support through an Otto-Hahn fellowship of the Max-Planck-Gesellschaft.

Appendix A. A microscopic description of ATPase

Here, we define the relevant properties of an ATPsynthase molecule via an Onsager theory. The fluxes that characterize the motion of ATPsynthase are the water current j , the proton current j_H , the ATP consumption rate r and the relative rotational velocity ω . If we denote by ω_1 and ω_2 the frequencies (measured in the laboratory reference frame) of the stalk and of the F_0 -part, respectively, the relative rotation velocity between the two parts is $\omega \equiv \omega_1 - \omega_2$. The conjugate forces to these fluxes are the chemical-potential difference of the protons between the two sides of the membrane $\Delta\mu_H$, the difference in chemical potential between ATP and its hydrolysis products $\Delta\mu_{\text{ATP}}$, the pressure difference across the membrane δP and the torque τ exerted on the stalk. ATPsynthase can be fully characterized by writing linear relations between the fluxes and the conjugate forces via an Onsager matrix

$$\omega = \alpha_H \Delta\mu_H + \alpha_{\text{ATP}} \Delta\mu_{\text{ATP}} + \nu \tau, \quad (\text{A.1})$$

$$j_H = \mu_H \Delta\mu_H + k \delta P + \alpha_H \tau, \quad (\text{A.2})$$

$$j = k \Delta\mu_H + \lambda \delta P, \quad (\text{A.3})$$

$$r = \alpha_{\text{ATP}} \tau + \Lambda \Delta\mu_{\text{ATP}}. \quad (\text{A.4})$$

The Onsager coefficients are the permeabilities k, λ and the response functions $\nu, \mu_H, \alpha_H, \alpha_{\text{ATP}}$, and Λ . In writing these equations we have made the simplifying assumptions that δP does not induce rotation, that j_H does not depend on $\Delta\mu_{\text{ATP}}$ and that r does not depend on δP and $\Delta\mu_H$. The off-diagonal coefficients of the Onsager matrix are equal in this linear theory.

Appendix B. Hydrodynamics of a motor in a viscous membrane

In this appendix, we solve the coupled hydrodynamic equations for the bulk fluid and the membrane containing a dipolar or a monopolar motor.

For dipolar motors and a force density given by equation (6), the Stokes equation reads, for $z > 0$ in \mathbf{q} -space,

$$-\eta q^2 \mathbf{v}(\mathbf{q}, z) + \eta \frac{d^2}{dz^2} \mathbf{v}(\mathbf{q}, z) + \mathbf{f}(\mathbf{q}, z) = 0; \quad (\text{B.1})$$

for $z < 0$,

$$-\eta q^2 \mathbf{v}(\mathbf{q}, z) + \eta \frac{d^2}{dz^2} \mathbf{v}(\mathbf{q}, z) = 0; \quad (\text{B.2})$$

and for $z = 0$, the two-dimensional Stokes equation is given by

$$-\eta_m q^2 \mathbf{v}(\mathbf{q}, 0) + \mathbf{f}_0(\mathbf{q}) + \eta \left. \frac{\partial \mathbf{v}}{\partial z} \right|_{z=0^+} - \eta \left. \frac{\partial \mathbf{v}}{\partial z} \right|_{z=0^-} = 0. \quad (\text{B.3})$$

These equations have to be solved subject to the boundary condition

$$\eta \left. \frac{\partial \mathbf{v}}{\partial z} \right|_{z=d^+} - \eta \left. \frac{\partial \mathbf{v}}{\partial z} \right|_{z=d^-} = -\mathbf{f}_0(\mathbf{q}). \quad (\text{B.4})$$

Equations (B.1) and (B.2) imply the ansatz

$$\begin{aligned} \mathbf{v}(\mathbf{q}, z) &= \mathbf{A} e^{qz} && \text{for } z < 0, \\ \mathbf{v}(\mathbf{q}, z) &= \mathbf{B} e^{qz} + \mathbf{C} e^{-qz} && \text{for } 0 < z < d, \\ \mathbf{v}(\mathbf{q}, z) &= \mathbf{D} e^{-qz} && \text{for } z > d. \end{aligned} \quad (\text{B.5})$$

Then, equations (B.3) and (B.4) together with the continuity of \mathbf{v} yield, for $d/z \ll 1$,

$$\mathbf{A} = \mathbf{f}_0(\mathbf{q}) \frac{d}{2\eta(1+ql)}, \quad (\text{B.6})$$

$$\mathbf{B} = -\mathbf{f}_0(\mathbf{q}) \frac{1-qd}{2\eta q}, \quad (\text{B.7})$$

$$\mathbf{C} = \mathbf{f}_0(\mathbf{q}) \frac{1+ql-q^2 dl}{2\eta q(1+ql)}, \quad (\text{B.8})$$

$$\mathbf{D} = -\mathbf{f}_0(\mathbf{q}) \frac{d(1+2ql)}{2\eta(1+ql)}, \quad (\text{B.9})$$

with $l \equiv \eta_m/2\eta$.

Similarly, for monopolar motors in a membrane, equations (B.2) and (B.3) have to be fulfilled for $z \neq 0$ and $z = 0$, respectively. Here, the ansatz

$$\mathbf{v}(\mathbf{q}, z) = \mathbf{A} e^{-q|z|} \quad (\text{B.10})$$

leads to

$$\mathbf{A} = \mathbf{f}_0(\mathbf{q}) \frac{1}{2\eta q(1+ql)}. \quad (\text{B.11})$$

References

1. B. Alberts *et al.*, *The Molecular Biology of the Cell*, 4th edition (Garland, New York, 2002).
2. M. Yoshida, E. Muneyuki, T. Hisabori, *Nat. Rev. Mol. Cell. Biol.* **2**, 669 (2001).
3. P.D. Boyer, *Biochim. Biophys. Acta* **1140**, 215 (1993).
4. J.P. Abrahams, A.G. Leslie, R. Lutter, J.E. Walker, *Nature* **370**, 621 (1994).
5. H. Noji, R. Yasuda, M. Yoshida, K. Kinoshita jr., *Nature* **386**, 299 (1997).
6. J.R. Blake, *Math. Meth. Appl. Sci.* **24**, 1469 (2001).
7. S. Nonaka *et al.*, *Cell* **95**, 829 (1998).

8. S. Gueron *et al.*, Proc. Natl. Acad. Sci. USA **94**, 6001 (1997).
9. S. Nonaka, H. Shiratori, Y. Saijoh, H. Hamada, Nature **418**, 96 (2002).
10. C.J. Tabin, K.J. Vogan, Genes Develop. **17**, 1 (2003).
11. J. McGrath *et al.*, Cell **114**, 61 (2003).
12. H. Hamada, C. Meno, D. Watanabe, Y. Saijoh, Nat. Rev. Mol. Cell. Biol. **3**, 103 (2001).
13. H. Liu *et al.*, Nat. Mater. **1**, 173 (2002).
14. R.K. Soong *et al.*, Science **290**, 1555 (2000).
15. J. Prost, R. Bruinsma, Europhys. Lett. **33**, 321 (1996); see also A.W.C. Lau *et al.*, cond-mat/0309510 (2003).
16. See, *e.g.*, R. Lipowsky, Nature **349**, 475 (1991) and U. Seifert, Adv. Phys. **46**, 13 (1997) for reviews.
17. J. Prost, J.-B. Manneville, R. Bruinsma, Eur. Phys. J. B **1**, 465 (1998).
18. S. Ramaswamy, J. Toner, J. Prost, Phys. Rev. Lett. **84**, 3494 (2000).
19. J.-B. Manneville, P. Bassereau, D. Lévy, J. Prost, Phys. Rev. Lett. **82**, 4356 (1999).
20. J.-B. Manneville, P. Bassereau, S. Ramaswamy, J. Prost, Phys. Rev. E **64**, 021908 (2001).
21. S. Levin, R. Korenstein, Biophys. J. **60**, 733 (1991).
22. S. Tuvia *et al.*, Proc. Natl. Acad. Sci. USA **94**, 5045 (1997).
23. F. Brochard, J.-F. Lennon, J. Phys. **36**, 1035 (1975).
24. B.A. Grzybowski, H.A. Stone, G.M. Whitesides, Nature **405**, 1033 (2000).
25. B.A. Grzybowski, X. Jiang, H.A. Stone, G.M. Whitesides, Phys. Rev. E **64**, 011603 (2001).
26. P. Galajda, P. Ormos, Appl. Phys. Lett. **80**, 4653 (2002).
27. P. Lenz, J.-F. Joanny, F. Jülicher, J. Prost, Phys. Rev. Lett., **91**, 108104 (2003).
28. R. Yasuda *et al.*, Cell **93**, 1117 (1998).
29. K. Kinosita jr., R. Yasuda, H. Noji, S. Ishiwata, M. Yoshida, Cell **93**, 21 (1998).
30. L.D. Landau, E.M. Lifshitz, *Hydrodynamics* (Pergamon, New York, 1959).
31. I.S. Gradshteyn, I.M. Ryzik, *Table of Integrals, Series and Products*, 5th edition (Academic Press, San Diego, 1994).
32. C. Barentin *et al.*, J. Fluid Mech. **397**, 331 (1999).
33. J.D. Jackson, *Classical Electrodynamics* (John Wiley, New York, 1999).
34. E.B. Sonin, Rev. Mod. Phys. **59**, 87 (1987).
35. G.K. Batchelor, *An Introduction to Fluid Dynamics* (Cambridge University Press, Cambridge, 2000).
36. It should be emphasized that our analysis is only valid for $N > 2$. For $N = 2$, the motors simply rotate around their center of mass and their interaction has no radial component. However, the presence of additional motors gives rise to a radial interaction which, in general, is repulsive.
37. J.M. Kosterlitz, D.J. Thouless, J. Phys. C **6**, 1181 (1973).
38. S.I. Rubinow, J.B. Keller, J. Fluid Mech. **11**, 447 (1961).
39. P. Brunn, Rheol. Acta **15**, 163 (1976).
40. Following the discussion given in reference [20], a force quadrupole is the simplest force distribution which is consistent with the rotational motion of the motor and the requirement that no external force is present.